

Article

Self-Assembly Heterometallic Cu-Ln Complexes: Synthesis, Crystal Structures and Magnetic Characterization

Shaoliang Zhang ^{1,*}, Ruili Du ¹, Xiufang Fan ¹, Xinhua Zhao ², Yanlan Wang ^{1,*} and Shanshan Li ^{3,*}

¹ Institution of Functional Organic Molecules and Materials, School of Chemistry and Chemical Engineering, Liaocheng University, Liaocheng 252059, China

² Department of Chemistry, South University of Science and Technology of China, Shenzhen 518055, China

³ School of Geography and Environment, Liaocheng University, Liaocheng 252059, China

* Correspondence: zhangshaoliang@lcu.edu.cn (S.Z.); wangyanlan@lcu.edu.cn (Y.W.); lishanshan@lcu.edu.cn (S.L.)

Abstract: Using N₂O₄ donor symmetric ligand H₂L and dca co-ligand, two new isostructural dinuclear Cu^{II}-Ln^{III} complexes [Cu(Cl)(L)Ln(NO₃)(CH₃OH)(H₂O)(dca)] [Ln=Ho (**1**_{CuHo}), Gd (**2**_{CuGd})] [H₂L = 6,6'-((1E,1'E)-(ethane-1,2-diylbis(azaneylylidene))bis(methaneylylidene))bis(2-methoxyphenol); dca=dicyanamide] were designed, synthesized and studied. In the two isostructural compounds, the geometric environment around the nine-coordinated Ln(III) ions is muffin, whereas the geometry of the penta-coordinated Cu(II) ions is square pyramid. The magnetic properties of both complexes were also studied. Direct current magnetic susceptibility measurements indicate ferromagnetic interactions between the Cu(II) ion and Gd(III) ion in complex **2**_{CuGd}. Alternating current (ac) magnetic measurements indicate that complex **1**_{CuHo} displays slow magnetic relaxation behaviour.

Keywords: Cu-Ln coordination compounds; X-ray diffraction; magnetism



Citation: Zhang, S.; Du, R.; Fan, X.; Zhao, X.; Wang, Y.; Li, S. Self-Assembly Heterometallic Cu-Ln Complexes: Synthesis, Crystal Structures and Magnetic Characterization. *Crystals* **2023**, *13*, 535. <https://doi.org/10.3390/cryst13030535>

Academic Editors: Giuseppe Greco and Anup Paul

Received: 29 January 2023

Revised: 22 February 2023

Accepted: 16 March 2023

Published: 21 March 2023



Copyright: © 2023 by the authors. Licensee MDPI, Basel, Switzerland. This article is an open access article distributed under the terms and conditions of the Creative Commons Attribution (CC BY) license (<https://creativecommons.org/licenses/by/4.0/>).

1. Introduction

Molecule-based magnets [1–5], which are widely applied in molecular spintronics [6–8], quantum computations [9–11], and as magneto luminescent materials [12], have gained much attention in the field of functional molecular materials. Among these, heterometallic 3d-4f polynuclear complexes make up one of the most interesting research topics [13–16]. In these type of complexes, the 4f ions provide large ground state magnetic moments and magnetic anisotropy, whereas the 3d ions take part in magnetic coupling interactions. Single-ion anisotropy [17–22] and magnetic coupling interactions [23–26] are crucial to the scale of the magnetization relaxation barrier. When there is a stronger 3d-4f magnetic exchange interaction, the quantum tunneling of magnetization (QTM) is effectively restrained, and large energy barriers, hysteresis loops and relaxation times can be observed [23,24]. Therefore, the 3d-4f metal combinations are more suitable for constructing low-dimensional molecular magnets (single molecule magnets, SMMs or single chain magnets, SCMs) [25–30].

Cu-Ln heterometallic complexes, among 3d-4f complexes, have encouraged special curiosity due to the ferromagnetic coupling interaction between the Cu(II) ion and the Ln(III) ion [31]. The [Cu₂Tb₂] complex, the first 3d-4f complex observed to have SMM properties, demonstrated that the magnetic interaction between the Cu(II) ion and the Tb(III) ion is critical to its SMM behavior [32]. In this regard, the SMM behavior of complexes in this category could be improved because the employment of Cu-Ln magnetic coupling interactions increases the ground state spin multiplicity.

Salen-type Schiff-base ligands obtained from salicylaldehyde derivatives and various diamines are typical materials frequently used to synthesize different 3d-4f complexes [33,34]. It can be easily tailored by changing the diamines or the substituent groups on aromatic rings. N₂O₂ donor ligands and N₂O₄ donor ligands are the two main types of Schiff-base ligands. N₂O₂ donor ligands can produce trinuclear 3d-4f complexes [35], whereas

N₂O₄ donor ligands can initiate the formation of di-, tri- and tetranuclear heterometallic complexes [13,28,33]. Furthermore, by varying 3d/4f/ligand molar ratios, tailoring Salen ligands and introducing different co-ligands, the structures of related 3d-4f complexes can be modulated [28]. Thus, it is compelling to research the structures and magnetic properties of 3d-4f-heterometallic-compound-based Salen ligands.

Dicyanamide (dca) has attracted extensive attention for the preparation of complexes with extended architectures because it is a utility ligand containing three nitrogen donor atoms, which make it possible to act as uni-, bi- and tridentate ligands in the area of coordination chemistry [36,37]. A dca ligand could be widely used to design SMMs [38], spin crossover complexes [39] and structural phase transition complexes [40].

Considering all the aspects stated above, we synthesized two Cu-Ln complexes [Ln=Ho(**1**_{CuHo}), Gd(**2**_{CuGd})]. The crystal structures and magnetic properties of the two new compounds were studied in this paper.

2. Experimental Section

2.1. Materials and Methods

Chemicals used were the finished product of Energy Chemical Company. H₂L was synthesized according to the method reported in reference [27]. Elements (e.g., C, H, N) in the two complexes were analysed with Elementar Vario MICRO analyzer (Langensfeld, Germany). IR data were collected on a Bruker Tensor 27 FT-IR spectrometer in the 4000–400 cm⁻¹ range (Billerica, MA, USA). Their magnetic properties were investigated on crushed crystal samples by means of a Quantum Design SQUID VSM magnetometer (San Diego, CA, USA). Experimental data were corrected for diamagnetism of the sample holder and that of the complexes according to Pascal's constants [41]. Powder X-ray diffraction (PXRD) of the two complexes were logged at 298 K on a Bruker D8 Advance diffractometer using Cu K α X-ray source (operated at 40 kV and 40 mA).

2.2. Synthesis

2.2.1. H₂L Synthesis

Hydroxy-3-methoxybenzaldehyde (20.00 mmol, 3.04 g) and ethylenediamine (10.00 mmol, 0.60 g) were mixed and dissolved in 50 mL ethanol. The above solution was refluxed for three hours and then cooled, the yellow crystal of H₂L ligand was formed. Yield: 90%. IR (KBr, cm⁻¹): 3425 (w), 2931 (w), 1632 (s), 1609 (m), 1467 (s), 1408 (m), 1249 (s), 1132 (w), 1080 (s), 1009 (m), 962 (s), 836 (m), 782 (m), 740 (s), 620 (m), 521 (w), 439 (w).

2.2.2. Complex **1**_{CuHo} Synthesis

A mixture of H₂L (32.8 mg, 0.100 mmol) and Cu(NO₃)₂·3H₂O (24.2 mg, 0.100 mmol) was dissolved in 3 mL of methanol, and mixed with a solution of HoCl₃·6H₂O (37.9 mg, 0.100 mmol) in 3 mL of CH₃OH-CH₃CN with *v/v* = 1:1). After a 30 min stir of the above solution, a 3 mL methanol solution containing NaN(CN)₂ (8.90 mg, 0.100 mol) was added. Then, it was filtered, and put into a test tube. Thus, diethyl ether vapor could be able to diffuse into the test tube. X-ray-suitable deep brown needle crystals were formed in the following seven days. Mass yield: 57%. Elemental analysis (%) calculated for C₂₂H₂₈N₆O₁₀ClCuHo: C, 33.0; H, 3.5; N, 10.5. Found: C, 33.1; H, 3.4; N, 10.6. IR (KBr, cm⁻¹): 3405 (w), 2311 (m), 2270 (m), 2218 (m), 2154 (s), 1636 (s), 1607 (s), 1558 (w), 1473 (m), 1456 (w), 1385 (w), 1281 (m), 1242 (m), 1222 (m), 1170 (w), 1078 (m), 1042 (w), 979 (w), 956 (w), 854 (m), 781 (w), 737 (m), 646 (w), 617 (w), 510 (w).

2.2.3. Complex **2**_{CuGd} Synthesis

Complex **2**_{CuGd} deep brown crystals were prepared following a similar procedure as that of complex **1**_{CuHo} using GdCl₃·6H₂O (37.1 mg, 0.100 mmol) instead of HoCl₃·6H₂O. Mass yield: 60%. Elemental analysis (%) calculated for C₂₂H₂₈N₆O₁₀ClCuGd: C, 33.3; H, 3.6; N, 10.6. Found: C, 33.4; H, 3.5; N, 10.6. IR (KBr, cm⁻¹): 3404 (w), 2269 (m), 2222 (m), 2162 (s), 1639 (s), 1609 (s), 1559 (w), 1473 (m), 1458 (w), 1386 (w), 1285 (m), 1241 (m), 1223 (s),

1171 (w), 1109 (m), 1077 (m), 1041 (w), 974 (m), 956 (w), 855 (m), 780 (w), 737 (s), 644 (m), 613 (w), 526 (m).

2.3. X-ray Crystallography

All reflections for single crystals of the complex **1**_{CuHo} and complex **2**_{CuGd} were collected at room temperature on a Bruker Apex II CCD detector with monochromated Mo K α ($\lambda = 0.71073 \text{ \AA}$) radiation. The structures of the two complexes were solved by direct method and refined by full-matrix least-squares method on F^2 through the SHELXTL software package [42–45]. The final crystallographic data and refinement parameters of the two complexes are listed in Table 1, and the data of selected bond distances and angles are listed in Tables S1 and S2.

Table 1. Crystallographic data for the two complexes.

Complex	1	2
Formula	C ₂₂ H ₂₈ N ₆ O ₁₀ ClCuHo	C ₂₂ H ₂₈ N ₆ O ₁₀ ClCuGd
M	800.42	792.74
Crystal system	Monoclinic	Monoclinic
Space group	<i>P</i> 21/ <i>n</i>	<i>P</i> 21/ <i>n</i>
<i>a</i> [Å]	8.8038(6)	8.8191(7)
<i>b</i> [Å]	16.3659(12)	16.5598(14)
<i>c</i> [Å]	19.8889(13)	20.0787(18)
α [°]	90	90
β [°]	91.5570(10)	91.748(2)
γ [°]	90	90
<i>V</i> [Å ³]	2864.6(3)	2931.0(4)
<i>Z</i>	4	4
ρ_{calcd} (g cm ^{−3})	1.856	1.797
<i>T</i> /K	298(2)	298(2)
<i>F</i> (000)	1580	1568
Crystal size (mm)	0.48 × 0.42 × 0.40	0.45 × 0.40 × 0.38
Reflections collected	13,358	13,751
Independent reflections	4984	5137
<i>R</i> _{int}	0.1262	0.1758
GOF	0.865	0.788
<i>R</i> ₁ ^a , <i>wR</i> ₂ ^b (<i>I</i> > 2 σ (<i>I</i>))	0.0901, 0.1761	0.0822, 0.1644

$$^a R_1 = \sum ||F_o| - |F_c|| / \sum |F_o| \quad ^b wR_2 = \{ \sum [w(F_o^2 - F_c^2)^2] / \sum [w(F_o^2)^2] \}^{1/2}.$$

3. Results and Discussion

3.1. IR Spectra

In the IR spectra, the strong absorption bands at 2154 cm^{−1} for complex **1**_{CuHo} and 2162 cm^{−1} for complex **2**_{CuGd} can be ascribed to the terminal ligands. One sole sharp peak can be observed at 1636 cm^{−1} (complex **1**_{CuHo}) and 1639 cm^{−1} (complex **2**_{CuGd}) for $\nu_{\text{C=N}}$ stretching, which indicates that the H₂L ligands have a symmetrical nature. The absorption peaks at 510 cm^{−1} for complex **1**_{CuHo} and 526 cm^{−1} for complex **2**_{CuGd} can be attributed to the stretching vibrations of metal–oxygen or metal–nitrogen.

3.2. Crystal Structure Descriptions

The two complexes are isostructural and display similar dinuclear [Cu^{II}LLn^{III}] structures with a symmetric ligand (H₂L), where Ln stands for Ho in complexes **1**_{CuHo} and Gd in complexes **2**_{CuGd}. The two complexes crystallized in the monoclinic space group with *Z* = 4. Here, we describe complex **1**_{CuHo} as a representative structure (Figure 1). On this molecule level, the central Ho(III) ion was coordinated to L^{2−} via two μ_2 -phenoxido oxygen atoms (O1, O2) and two methoxy oxygen atoms (O3, O4). Along with this, one chelating bidentate nitrate ligand (O5, O6), one methanol molecule (O8), one water molecule (O9) and one terminal dca ligand (N4) make the Ho(III) centre nine-coordinated. The Cu(II) ion

is five-coordinated surrounded by the four atoms (O1, O2, N1, N2) from the L^{2-} ligands and one axial Cl1 atom.

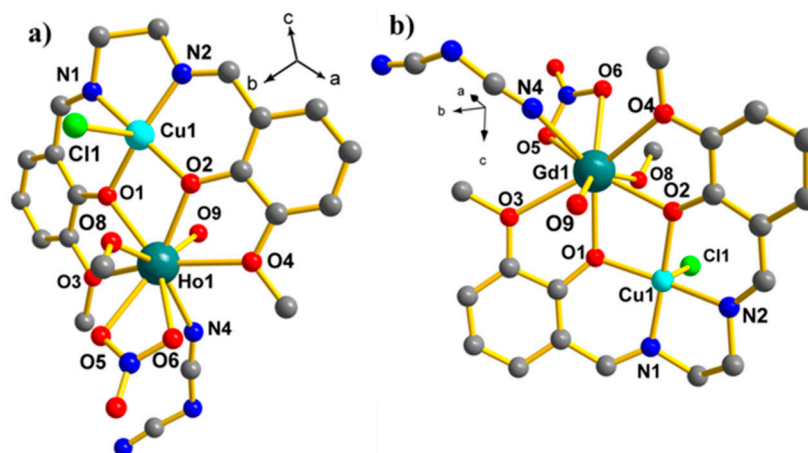


Figure 1. The crystal structure of complex 1_{CuHo} (a), complex 2_{CuGd} (b).

We calculated the continuous shape measures (CShM) to estimate the coordination geometry of the metal ions (Ln and Cu in Figure 2) through the SHAPE 2.1 software [46]. The results (Tables S3 and S4, ESI†) show that the lowest CShM values for Ln1 are 2.243 for complex 1_{CuHo}, and 2.298 for complex 2_{CuGd}, which indicates the environment of Ln is a muffin geometry; the CShM values for Cu1 are 1.687 for complex 1_{CuHo}, and 1.640 for complex 2_{CuGd}, which indicates the environment of Cu is a square pyramid geometry. The bond lengths of Cu–O/N lie in the ranges of 1.888(14)–1.962(12) Å and the bond lengths of Ln–O/N range from 2.316(10) to 2.641(10) Å, which fall in the normal range compared to the other heterometallic dinuclear Cu^{II}Ln^{III} (Ln = Tb and Dy) compounds originating from N2O3 donor unsymmetrical ligands [29,30] and N2O4 donor symmetrical ligands [27].

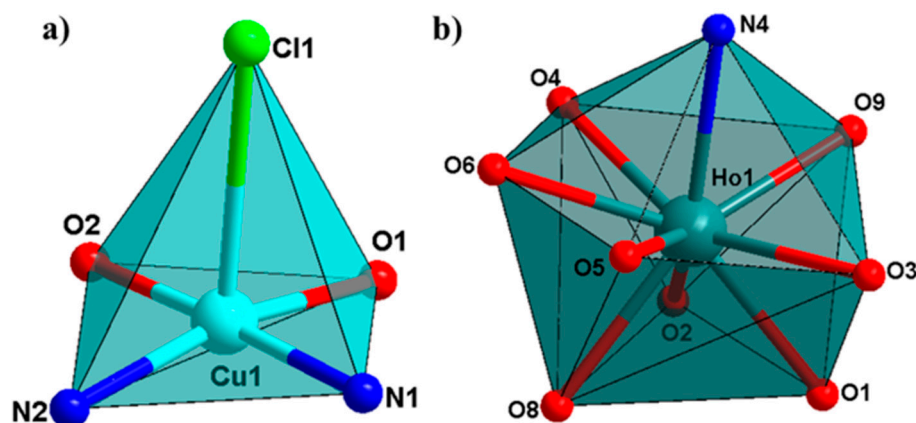


Figure 2. The coordination geometries of Cu(II) (a) and Ho(III) (b) in complex 1.

As is well noted, hydrogen bonding and π - π interactions are crucial to construct and stabilize supramolecular structures. In complex 1_{CuHo}, the monomer is connected into a chain through O–H \cdots Cl hydrogen bonds' interaction along the a-axis direction. Furthermore, the two neighboring chains are interlinked into a supramolecular 2-D layer in the *ab* plane through the π - π stacking between the two phenyl rings defined by C1 \cdots C6 and C11 \cdots C16 from the H₂L ligands. (Figure 3, Table 2)

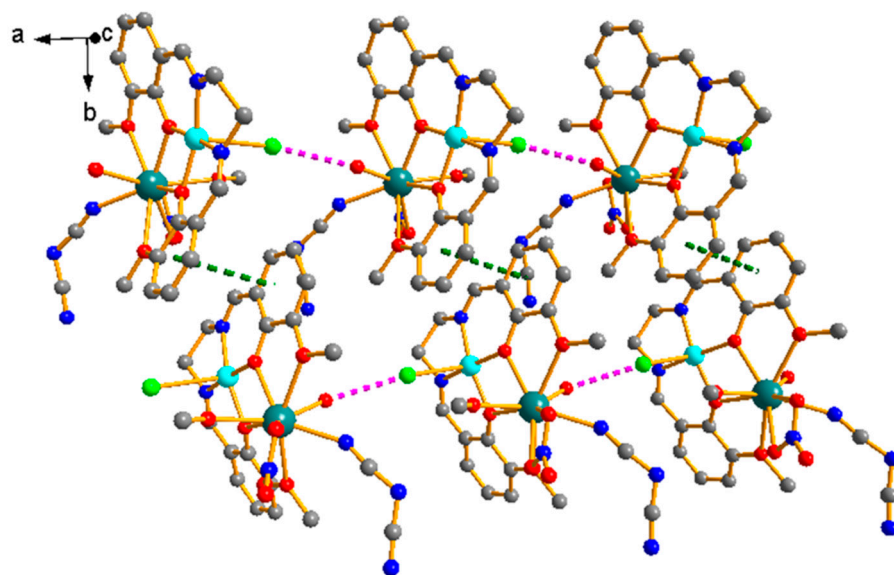


Figure 3. The 2-D layer built through hydrogen bond interactions and π - π stacking in complex 1.

Table 2. Hydrogen bonding and π - π interactions [\AA] for the two complexes.

Complex	D...A	D(D...A)/ \AA
complex 1 _{CuHo}	O9...Cl1 ^a	3.023(2)
	π ... π ^b	3.763(2)
complex 2 _{CuGd}	O9...Cl1 ^a	3.056(2)
	π ... π ^b	3.872(2)

Symmetry codes: ^a: $1 + x, y, z$; ^b: $1.5 - x, 0.5 + y, 0.5 - z$.

3.3. Magnetic Properties

The temperature-dependent magnetic susceptibility data of the polycrystalline complexes 1_{CuHo}-2_{CuGd} were determined in the temperature interval of 2–300 K under an applied direct current (DC) 1000 Oe field. (Figure 4) For the complex 1_{CuHo}, the value of $\chi_M T$ is $14.22 \text{ cm}^3 \text{ mol}^{-1} \text{ K}$ under room temperature, which is close to the theoretical value $14.445 \text{ cm}^3 \text{ mol}^{-1} \text{ K}$. (Cu: $g = 2.0, S = 1/2$; Ho: $g = 5/4, J = 8$). Upon cooling from 300 K, the $\chi_M T$ decreases monotonically, which could be attributed to the depopulation of the Zeeman effect and possible weak antiferromagnetic interactions between the spin centers.

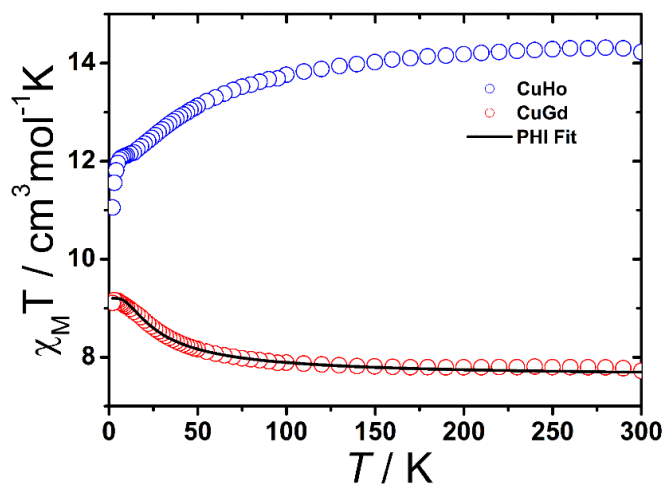


Figure 4. Temperature-dependent magnetic susceptibility data for complexes 1–2, solid lines show the best fits to the appropriate model.

The value of $\chi_M T$ for complex **2**_{CuGd} at 300 K is $7.72 \text{ cm}^3 \text{ mol}^{-1} \text{ K}$, in line with the expected value for one magnetically isolated $\text{Cu}^{\text{II}}\text{Gd}^{\text{III}}$ unit $8.255 \text{ cm}^3 \text{ mol}^{-1} \text{ K}$ (Cu: $g = 2.0$, $S = 1/2$; Gd: $g = 2$, $J = 7/2$). In contrast to complex **1**_{CuHo}, the value of $\chi_M T$ for complex **2**_{CuGd} gradually increased up towards the maximum ($9.16 \text{ cm}^3 \text{ mol}^{-1} \text{ K}$ at 5.0 K), which indicated the presence of a major ferromagnetic interaction through Gd-O-Cu, and then decreased to $9.10 \text{ cm}^3 \text{ mol}^{-1} \text{ K}$ at 2.0 K. This slight drop at the lower temperature indicated the existence of the intermolecular antiferromagnetic coupling [47]. The neighboring interdimer Gd···Gd distances were 8.819 \AA along the b axis. Compared to the literature, the Gd···Gd distances are short enough to give an antiferromagnetic interaction. [47]. This can be described by a dinuclear model with a spin Hamiltonian as $H = -2J_{\text{Cu}}S_{\text{Cu}}S_{\text{Gd}}$. The dc magnetic data were fitted using PHI program [48], in which the best fit presented $J = 2.97 \text{ cm}^{-1}$, $g_{\text{Cu}} = 1.92$, and $g_{\text{Gd}} = 1.92$ for complex **2**, revealing that there is ferromagnetic $\text{Cu}^{\text{II}}\text{-Gd}^{\text{III}}$ interaction in complex **2**.

Several complexes with a magneto-structural relationship, where the Cu(II)-Gd(III) exchange interaction parameter is depicted as a function of Cu-O-Gd bond angles, have been reported [28]. Generally, the ferromagnetic interaction can be observed between heavy Ln(III) and Cu(II). Alternatively, with the increase in the number of unpaired electrons in the 4f orbitals, the probability of AF interaction between the $d_{x^2-y^2}$ orbital of Cu^{II} and the magnetic orbitals of the 4f shell also goes up [30]. Thus, moving from Tb^{III} to Er^{III} , the AF contribution is gradually increased. (Table 3, The complexes **3**_{CuTb} and **4**_{CuDy} are isostructural with the current complexes **1**_{CuHo} and **2**_{CuGd}.)

Table 3. Geometrical features and magnetic parameters of Cu-Ln bimetallic complexes.

Complex	Cu-Ln Interaction	Cu-O _{phenol} -Ln Bridging Angle (°)	Cu-O _{phenol} Bond Length (Å)	Ln-O _{phenol} Bond Length (Å)	SMM Behavior under Zero DC Field	Ref
1 _{CuHo}	antiferromagnetic	105.15/104.06	1.929/1.938	2.316/2.338	yes	This work
2 _{CuGd}	ferromagnetic	104.96/105.41	1.948/1.925	2.366/2.375	no	This work
3 _{CuTb}	ferromagnetic	105.43/104.48	1.907/1.943	2.334/2.327	yes	27
4 _{CuDy}	ferromagnetic	104.52/105.42	1.942/1.915	2.328/2.328	no	27

The field-dependent magnetization curves of these compounds at 2 K were measured at the range of 0–70 KOe. (Figure 5). The experimental magnetizations at 7 T are 6.22 and $7.19 \mu_B$ for complexes **1**_{CuHo}–**2**_{CuGd}, respectively (Table 4). The magnetization value of complex **1**_{CuHo} was apparently lower than the saturated magnetization value, which can be explained by the strong magnetic anisotropy of the Ho(III) ion.

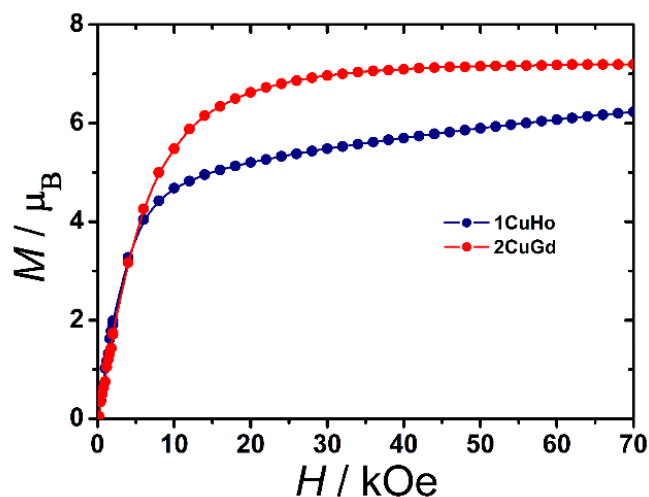
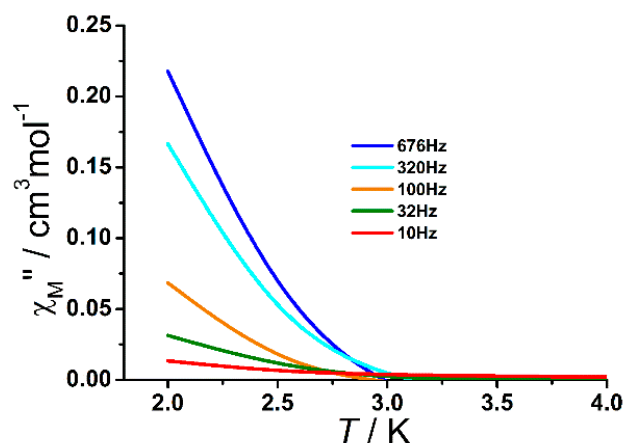


Figure 5. Isothermal magnetization of complexes **1**–**2** at 2 K with DC field of up to 70 KOe.

Table 4. Experimental and theoretical values of $\chi_M T$ at room temperature and the saturation magnetization M (70 KOe, 2 K) for the two compounds.

Complex	Ground State of Ln	$\chi_M T / \text{cm}^3 \text{mol}^{-1} \text{K}$ (Theoretical)	$\chi_M T / \text{cm}^3 \text{mol}^{-1} \text{K}$ (Observed)	M / μ_B (Theoretical)	M / μ_B (Observed)
1 _{CuHo}	⁵ I ₈	14.445	14.22	11	6.22
2 _{CuGd}	⁸ S _{7/2}	8.255	7.72	8	7.19

The observation of an out-of-phase χ_M'' ac susceptibility signal is one of the important characteristics of an SMM. Thus, alternating current (ac) magnetic susceptibilities were performed in the temperature range of 2.0–6.0 K without the applied DC field at different frequencies to analyse the dynamics of the magnetization of the two complexes. As can be seen from Figure 6, complex **1**_{CuHo} exhibited an out-of-phase χ_M'' signal below 3.0 K. Although no maximum was observed down to 2.0 K, an obvious frequency dependence of the χ_M'' signal was shown to be consistent with the SMM behaviour. It can be seen from Figure S1 that there were no observable out-of-phase signals down to 2.0 K, which rules out the SMM behaviour of complex **2**_{CuGd}.

**Figure 6.** Frequency dependence of the out-of-phase χ_M'' ac magnetic susceptibility versus T for complex **1**_{CuHo} measured under $H_{ac} = 2$ Oe and $H_{dc} = 0$ Oe.

This variance in SMM properties for these complexes under zero field can be interpreted through the spin parity effect of the 3d-4f ions in the ferro-/antiferromagnetically-coupled complexes (i.e., Kramer's molecules, complex **1**_{CuHo} and complex **3**_{CuTb}, are likely to display SMM behaviours).

4. Conclusions

Two Cu(II)-Ln(III) (Ln=Ho and Gd) complexes were synthesized. The X-ray crystal structures revealed that they are both isostructural and display a similar dinuclear structure, where the Ln(III) ion was nine-coordinated and the Cu(II) ion was five-coordinated. Magnetic studies revealed that the Cu(II) and Gd(III) centers show a ferromagnetic interaction, and the Cu(II) and Ho(III) show an antiferromagnetic interaction. Complex **1**_{CuHo} exhibits a slow magnetic relaxation behaviour below 3K at zero field. They may provide an experimental basis for expanding the 3d-4f compound families and enlightening further studies on the magnetic property of 3d-4f compounds. In future, we will continue to study the effect of diverse 3d-4f structures on magnetic properties in depth. Hopefully, we will be able to effectually regulate magnetic properties by accommodating the N2O3 donor ligand with the absence of symmetry elements.

Supplementary Materials: The following supporting information can be downloaded at: <https://www.mdpi.com/article/10.3390/cryst13030535/s1>.

Author Contributions: S.Z. Methodology, Software, Supervision, Writing-original draft. R.D. Experimental and Data curation. X.F. Experimental and Data curation. X.Z. Software and Data curation. Y.W. Reviewing and Editing. S.L. Reviewing and Editing. All authors have read and agreed to the published version of the manuscript.

Funding: The research was funded by Natural Science Foundation of Shandong Province (grant number: ZR2016BB07) and National Natural Science Foundation of China (grant number: 21901097).

Data Availability Statement: The crystallographic data CCDC-2097679 (1), 2097680 (2) for this paper can be obtained free of charge from The Cambridge Crystallographic Data Centre via www.ccdc.cam.ac.uk/data_request/cif (accessed on 28 January 2023).

Acknowledgments: We thank to Introduction and Cultivation Program for Young Innovative Talents in Shandong Provincial Colleges and Universities (Innovation Team of Functional Organometallic Materials presided by Yanlan Wang).

Conflicts of Interest: The authors declare no conflict of interest.

References

1. Gao, S. Molecular Nanomagnets and Related Phenomena. In *Structure and Bonding*; Springer: Berlin/Heidelberg, Germany, 2015. [CrossRef]
2. Sessoli, R.; Gatteschi, D.; Caneschi, A.; Novak, M.A. Magnetic bistability in a metal-ion cluster. *Nature* **1993**, *365*, 141–143. [CrossRef]
3. Miller, J.S.; Gatteschi, D. (Eds.) Themed issue on Molecule-based Magnets. *Chem. Soc. Rev.* **2011**, *40*, 3053. [CrossRef]
4. Jiang, S.D.; Wang, B.W.; Su, G.; Wang, Z.M.; Gao, S. A Mononuclear Dysprosium Complex Featuring Single-Molecule-Magnet Behavior. *Angew. Chem. Int. Ed.* **2010**, *49*, 7448–7451. [CrossRef] [PubMed]
5. Guo, F.-S.; Day, B.M.; Chen, Y.-C.; Tong, M.-L. Magnetic hysteresis up to 80 kelvin in a dysprosium metallocene single-molecule magnet. *Science* **2018**, *362*, 1400–1403. [CrossRef] [PubMed]
6. Boganai, L.; Wersdorfer, W. Molecular spintronics using single-molecule magnets. *Nat. Mater.* **2008**, *7*, 179–186. [CrossRef]
7. Vincent, R.; Klyatskaya, S.; Ruben, M.; Wersdorfer, W.; Balestro, F. Electronic read-out of a single nuclear spin using a molecular spin transistor. *Nature* **2012**, *488*, 357–360. [CrossRef]
8. Woodruff, D.N.; Winpenny, R.E.P.; Layfield, R.A. Lanthanide Single-Molecule Magnets. *Chem. Rev.* **2013**, *113*, 5110–5148. [CrossRef]
9. Hill, S.; Edwards, R.S.; Aliaga-Alcalde, N.; Christou, G. Quantum Coherence in an Exchange-Coupled Dimer of Single-Molecule Magnets. *Science* **2003**, *302*, 1015–1018. [CrossRef]
10. Leuenberger, M.N.; Loss, D. Quantum computing in molecular magnets. *Nature* **2001**, *410*, 789–793. [CrossRef]
11. Gatteschi, D.; Sessoli, R. Quantum Tunneling of Magnetization and Related Phenomena in Molecular Materials. *Angew. Chem. Int. Ed.* **2003**, *42*, 268–297. [CrossRef] [PubMed]
12. Pointillart, F.; Le Guennic, B.; Cador, O.; Maury, O.; Ouahab, L. Lanthanide Ion and Tetrathiafulvalene-Based Ligand as a “Magic” Couple toward Luminescence, Single Molecule Magnets, and Magnetostructural Correlations. *Acc. Chem. Res.* **2015**, *48*, 2834–2842. [CrossRef]
13. Liu, K.; Shi, W.; Cheng, P. Toward heterometallic single-molecule magnets: Synthetic strategy, structures and properties of 3d–4f discrete complexes. *Coord. Chem. Rev.* **2015**, *289–290*, 74–122. [CrossRef]
14. Piquer, L.R.; Sañudo, E.C. Heterometallic 3d–4f single-molecule magnets. *Dalton Trans.* **2015**, *44*, 8771–8780. [CrossRef]
15. Costes, J.P.; Ladeira, S.M.; Vendier, L.; Maurice, R.; Wernsdorfer, W. Influence of ancillary ligands and solvents on the nuclearity of Ni–Ln complexes. *Dalton Trans.* **2019**, *48*, 3404–3414. [CrossRef]
16. Dhers, S.; Costes, J.P.; Guionneau, P.; Paulsen, C.; Vendier, L.; Sutter, J.P. On the importance of ferromagnetic exchange between transition metals in field-free SMMs: Examples of ring-shaped hetero-trimetallic [(LnNi₂){W(CN)₈}₂] compounds. *Chem. Commun.* **2015**, *51*, 7875–7878. [CrossRef] [PubMed]
17. Liu, K.; Zhang, X.-J.; Meng, X.-X.; Shi, W.; Cheng, P.; Powell, A.K. Constraining the coordination geometries of lanthanide centers and magnetic building blocks in frameworks: A new strategy for molecular nanomagnets. *Chem. Soc. Rev.* **2016**, *45*, 2423–2439. [CrossRef] [PubMed]
18. Day, B.M.; Guo, F.-S.; Layfield, R.A. Cyclopentadienyl Ligands in Lanthanide Single-Molecule Magnets: One Ring To Rule Them All? *Acc. Chem. Res.* **2018**, *51*, 1880–1889. [CrossRef]
19. Zhu, Z.; Guo, M.; Li, X.L.; Tang, J. Molecular magnetism of lanthanide: Advances and perspectives. *Coord. Chem. Rev.* **2019**, *378*, 350–364. [CrossRef]
20. Jia, J.H.; Li, Q.W.; Chen, Y.C.; Liu, J.L.; Tong, M.L. Luminescent single-molecule magnets based on lanthanides: Design strategies, recent advances and magneto-luminescent studies. *Coord. Chem. Rev.* **2019**, *378*, 365–381. [CrossRef]
21. Goodwin, C.A.P.; Ortu, F.; Reta, D.; Chilton, N.F.; Mills, D.P. Molecular magnetic hysteresis at 60 kelvin in dysprosocenium. *Nature* **2017**, *548*, 439. [CrossRef]

22. Bar, A.K.; Kalita, P.; Singh, M.K.; Rajaraman, G.; Chandrasekhar, V. Low-coordinate mononuclear lanthanide complexes as molecular nanomagnets. *Coord. Chem. Rev.* **2018**, *367*, 163–216. [[CrossRef](#)]
23. Li, J.; Wei, R.-M.; Pu, T.-C.; Cao, F.; Yang, L.; Han, Y.; Zhang, Y.-Q.; Zuo, J.-L.; Song, Y. Tuning quantum tunnelling of magnetization through 3d–4f magnetic interactions: An alternative approach for manipulating single-molecule magnetism. *Inorg. Chem. Front.* **2017**, *4*, 114–122. [[CrossRef](#)]
24. Mishra, A.; Wernsdorfer, W.; Parsons, S.; Christou, G.; Brechin, E.K. The search for 3d–4f single-molecule magnets: Synthesis, structure and magnetic properties of a [Mn^{III}Dy^{III}]₂ cluster. *Chem. Commun.* **2005**, *16*, 2086–2088. [[CrossRef](#)] [[PubMed](#)]
25. Cimpoesu, F.; Dahan, F.; Ladeira, S.; Ferbinteanu, M.; Costes, J.P. Chiral Crystallization of a Heterodinuclear Ni–Ln Series: Comprehensive Analysis of the Magnetic Properties. *Inorg. Chem.* **2012**, *51*, 11279–11293. [[CrossRef](#)]
26. Wen, H.-R.; Bao, J.; Liu, S.-J.; Liu, C.-M.; Zhang, C.-W.; Tang, Y.-Z. Temperature-controlled polymorphism of chiral Cu^{II}–Ln^{III} dinuclear complexes exhibiting slow magnetic relaxation. *Dalton Trans.* **2015**, *44*, 11191–11201. [[CrossRef](#)]
27. Zhang, S.L.; Fan, X.F.; Du, R.L.; Shen, B.W.; Song, X.D.; Wei, X.Q.; Li, S.S. Synthesis, crystal structures and magnetism of Cu^{II}Ln^{III} N₂O₄-donor coordination compounds involving dicyanamides. *Polyhedron* **2021**, *206*, 115336. [[CrossRef](#)]
28. Dey, A.; Bag, P.; Kalita, P.; Chandrasekhar, V. Heterometallic Cu^{II}–Ln^{III} complexes: Single molecule magnets and magnetic refrigerants. *Coord. Chem. Rev.* **2021**, *432*, 213707. [[CrossRef](#)]
29. Maity, S.; Bhunia, P.; Ichihashi, K.; Ishida, T.; Ghosh, A. SMM behaviour of heterometallic dinuclear Cu^{II}Ln^{III} (Ln = Tb and Dy) complexes derived from N₂O₃ donor unsymmetrical ligands. *New J. Chem.* **2020**, *44*, 6197–6205. [[CrossRef](#)]
30. Mahapatra, P.; Koizumi, N.; Kanetomo, T.; Ishida, T.; Ghosh, A. A series of Cu^{II}–Ln^{III} complexes of an N₂O₃ donor asymmetric ligand and a possible Cu^{II}–Tb^{III} SMM candidate in no bias field. *New J. Chem.* **2019**, *43*, 634–643. [[CrossRef](#)]
31. Shimada, T.; Okazawa, A.; Kojima, N.; Yoshii, S.; Nojiri, H.; Ishida, T. Ferromagnetic Exchange Couplings Showing a Chemical Trend in Cu–Ln–Cu Complexes (Ln = Gd, Tb, Dy, Ho, Er). *Inorg. Chem.* **2011**, *50*, 10555–10557. [[CrossRef](#)]
32. Osa, S.; Kido, T.; Matsumoto, N.; Re, N.; Pochaba, A.; Mrozinski, J. A Tetranuclear 3d–4f Single Molecule Magnet: [Cu^{II}L^{Tb}III(hfac)₂]₂. *J. Am. Chem. Soc.* **2004**, *126*, 420–421. [[CrossRef](#)]
33. Yang, X.P.; Jones, R.A.; Huang, S.M. Luminescent 4f and d-4f polynuclear complexes and coordination polymers with flexible salen-type ligands. *Coord. Chem. Rev.* **2014**, *273–274*, 63–75. [[CrossRef](#)]
34. Andruh, M. The exceptionally rich coordination chemistry generated by Schiff-base ligands derived from o-vanillin. *Dalton Trans.* **2015**, *44*, 16633–16653. [[CrossRef](#)]
35. Mahapatra, P.; Ghosh, S.; Koizumi, N.; Kanetomo, T.; Ishida, T.; Drew, M.G.B.; Ghosh, A. Structural variations in (CuL)₂Ln complexes of a series of lanthanide ions with a salen-type unsymmetrical Schiff base(H₂L): Dy and Tb derivatives as potential single-molecule magnets. *Dalton Trans.* **2017**, *46*, 12095–12105. [[CrossRef](#)] [[PubMed](#)]
36. Ohba, M.; Okawa, H. Synthesis and magnetism of multi-dimensional cyanide-bridged bimetallic assemblies. *Coord. Chem. Rev.* **2000**, *198*, 313–328. [[CrossRef](#)]
37. Batten, S.R.; Murray, K.S. Structure and magnetism of coordination polymers containing dicyanamide and tricyanomethanide. *Coord. Chem. Rev.* **2003**, *246*, 103–130. [[CrossRef](#)]
38. Colacio, E.; Ruiz, J.; Mota, A.J.; Palacios, M.A.; Ruiz, E.; Cremades, E.; Hänninen, M.M.; Sillanpää, R.; Brechin, E.K. Co^{II}Ln^{III} dinuclear complexes (Ln^{III} = Gd, Tb, Dy, Ho and Er) as platforms for 1,5-dicyanamide-bridged tetranuclear Co^{II}₂Ln^{III}₂ complexes: A magneto-structural and theoretical study. *C. R. Chim.* **2012**, *15*, 878–888. [[CrossRef](#)]
39. Roy, S.; Choubey, S.; Bhar, K.; Sikdar, N.; Costa, J.S.; Mitra, P.; Ghosh, B.K. Counter anion dependent gradual spin transition in a 1D cobalt(ii) coordination polymer. *Dalton Trans.* **2015**, *44*, 7774–7776. [[CrossRef](#)]
40. Xu, W.J.; Du, Z.Y.; Zhang, W.X.; Chen, X.-M. Structural phase transitions in perovskite compounds based on diatomic or multiautomic bridges. *CrystEngComm* **2016**, *18*, 7915–7928. [[CrossRef](#)]
41. Carlin, R.L. *Magnetochemistry*; Springer Press: Berlin/Heidelberg, Germany, 1986.
42. *SAINT Software Users Guide, Version 7.0*; Bruker Analytical X-Ray Systems: Madison, WI, USA, 1999.
43. Sheldrick, G.M. *SADABS, Version 2.03*; Bruker Analytical X-Ray Systems: Madison, WI, USA, 2000.
44. Sheldrick, G.M. *SHELXL-2014*; Program for the Solution of Crystal Structures; University of Göttingen: Göttingen, Germany, 2014.
45. Sheldrick, G.M. *SHELXT, Version 6.14*; Bruker AXS, Inc.: Madison, WI, USA, 2003.
46. Casanova, D.; Alemany, P.; Bofill, J.M.; Alvarez, S. Shape and Symmetry of Heptacoordinate Transition-Metal Complexes: Structural Trends. *Chem. Eur. J.* **2003**, *9*, 1281–1295. [[CrossRef](#)]
47. Kong, J.J.; Zhang, J.C.; Jiang, Y.X.; Tao, J.X.; Wang, W.Y.; Huang, X.C. Two-dimensional heterometallic Cu^{II}Ln^{III} (Ln = Tb and Dy) coordination polymers bridged by dicyanamides showing slow magnetic relaxation behaviour. *CrystEngComm* **2019**, *21*, 5145–5151. [[CrossRef](#)]
48. Chilton, N.F.; Anderson, R.P.; Turner, L.D.; Soncini, A.; Murray, K.S. PHI: A powerful new program for the analysis of anisotropic monomeric and exchange-coupled polynuclear d- and f-block complexes. *J. Comput. Chem.* **2013**, *34*, 1164–1175. [[CrossRef](#)] [[PubMed](#)]

Disclaimer/Publisher’s Note: The statements, opinions and data contained in all publications are solely those of the individual author(s) and contributor(s) and not of MDPI and/or the editor(s). MDPI and/or the editor(s) disclaim responsibility for any injury to people or property resulting from any ideas, methods, instructions or products referred to in the content.